Light Harvesting

DOI: 10.1002/anie.201202428

Nanopatterning of Mesoporous Inorganic Oxide Films for Efficient Light Harvesting of Dye-Sensitized Solar Cells**

Jeonghun Kim, Jong Kwan Koh, Byeonggwan Kim, Jong Hak Kim, and Eunkyoung Kim**

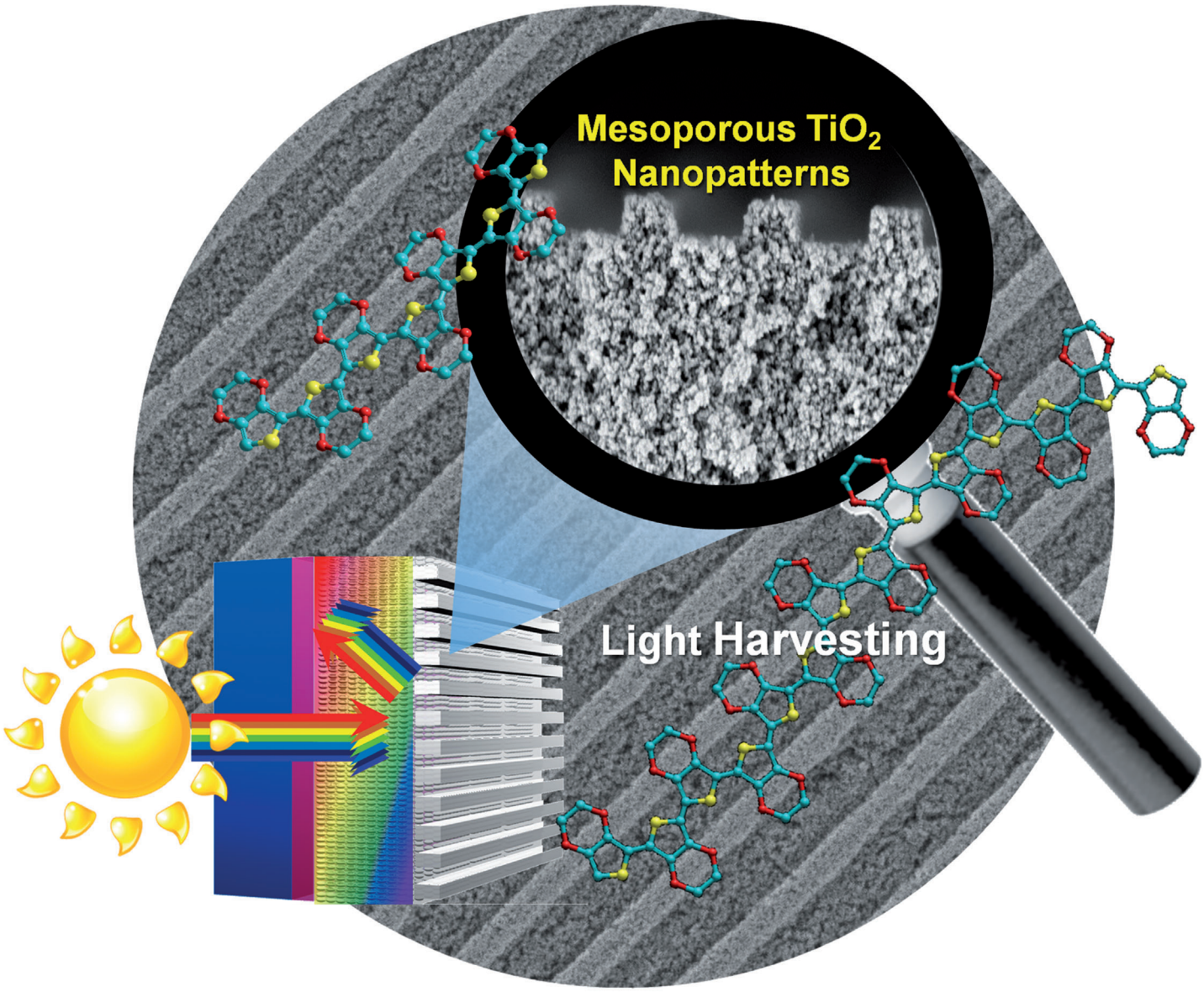

Nanopatterning, a renowned method for constructing photonic nanostructures, has received tremendous attention as a means of boosting the efficiency η in photovoltaics using enhanced light harvesting.[1,2] However, nanopatterning is limited owing to the specific fabrication method and characteristics of the component materials required for the photovoltaic applications.[3–8] Despite recent intensive efforts, facile nanopatterning methods and ideal nanophotonic structures for efficient light trapping have not been identified.

Nanocrystalline mesoporous titanium dioxide (TiO_2) is a core material in dye-sensitized solar cells (DSSCs) because sensitizer adsorption, electron transport, and recombination characteristics are directly influenced by its properties.[9] Thus, many efforts have been made to control the crystallinity, phase, particle size, surface area, interconnection between particles, and pore morphology of TiO_2 to increase the cell performance.[10–12] Considerable attention has also been directed toward developing sensitizing dyes,[13–16] electrolytes,[15–17] and efficient cell structures.[18–20] One of the most accessible and attainable routes for enhancing solar cell efficiency is to modify its optical design to improve the harvest of total incident light within the cell. Recently, many approaches have reported light-trapping techniques of DSSCs using photonic crystals,[5,21,22] plasmonic effects,[7] various nanostructuring processes,[8,23,24] and modified electrolytes.[25]

Although nanopatterning of the electrode for light trapping has been performed in polymer solar cells[1] and silicon solar cells,[2] the application of a universal method for DSSCs has not been reported, which is mainly due to difficulty in nanopatterning the dye-adsorbed mesoporous TiO_2 layer. There have been a few trials of TiO_2 nanopatterning using 1) solution synthesis of TiO_2[26] and 2) imprinting with high pressure and a fragile quartz stamp.[7] In solution synthesis, Hammond and Tokuhisa[26] observed an increased surface area effect of bulk TiO_2 (not TiO_2 nanoparticles (NPs)) by nanograting formation, but the efficiency was low ($\eta < 1.0\,\%$) owing to the thinness of the TiO_2 and the complex solution process. For the imprinting method, Grätzel and McGehee[7] reported direct nanopatterning of TiO_2 NPs from commercially available paste to produce disordered 600 nm dome arrays and nanopatterns, which were further coated with silver to promote the plasmonic effect. However, these two nanopatterning methods have not been used as a universal method for solar cells owing to their complex and expensive processes, low η, and difficulties in mass production. To this end, we developed a universal nanopatterning method for mesoporous inorganic oxide films, such as TiO_2, based on analysis by surface and material chemistry.

Herein, we present unprecedented universal nanopatterning that provides a facile process to produce the first large-area platform with well-arrayed nanopatterns of mesoporous inorganic oxide films at low cost using readily available pastes and elastomeric nanostamps. The application of the nanopattern resulted in approximately 40 % and 33 % enhancement of the short-circuit current (J_{sc}) and PCE (η), respectively, to afford a PCE of 7.03 % at 100 mW cm^{-2}, which is one of the highest values reported for N719-dye-based, iodine-free solid-state DSSCs (ssDSSCs) to date (Table 1). This nanopatterning technique will improve performance in any type of photovoltaic cells using mesoporous inorganic oxide films.

Table 1: Performances of the iodine-free ssDSSCs with and without a nanopattern on mesoporous TiO_2 photoelectrodes at 100 mW cm^{-2}.

DSSC	J_{sc} [mA cm^{-2}]	V_{oc} [mV]	FF [%]	η [%]
without nanopattern	13.8	639	60	5.29
with nanopattern	19.2	654	56	7.03

We prepared mesoporous TiO_2 films with a thickness of about 11 μm, 250 nm wide nanopatterns (period ca. 600 nm), and a large area cell (ca. 5.76 cm^2) without defects, and used the films as a photoelectrode in I_2-free ssDSSCs with highly conductive poly(3,4-ethylenedioxythiophene) (PEDOT, ca. 10 S cm^{-1}) as a hole-transporting material (HTM).[27,28] The overall procedure for fast and simple nanopatterning of TiO_2 photoelectrodes using an elastomeric polydimethylsiloxane (PDMS) nanostamp and available TiO_2 paste is shown in Figure 1. The most important property required for nanopatterning is the neutrality of the paste (see the Supporting Information, Figure S1a,b insets for pH tests). The use of an acidic paste generally results in the formation of thicker (> 10 μm) TiO_2 films without cracking or peeling-off owing to the closely-packed TiO_2 NPs, and thus most paste formulations contain an acid source. However, after patterning by the PDMS stamp, the calcined TiO_2 photoelectrode prepared with acidic paste became hydrophobic owing to the presence of unavoidable hydrophobic PDMS residues[29] that led to SiO_2 formation[30] on the surface. The calcined film exhibited strong evidence of hydrophobic Si–O–Si and Si–CH_3 groups (Supporting Information, Figure S2c) similar to those in PDMS ($CH_3[Si(CH_3)_2O]_nSi(CH_3)_3$). These peaks were attributed to the residues (including SiO_2 by thermal treatment[30]) of detached PDMS when removed in the patterning process, as shown in scanning electron microscopy (SEM) images (Supporting Information, Figure S2d,e). As the acidic paste modifies the surface of the PDMS stamp into OH functional groups, the stamp could be strongly bonded to the OH groups of TiO_2 nanoparticles under highly acidic condition (Support-

[*] Dr. J. Kim,[+] J. K. Koh,[+] B. Kim, Prof. Dr. J. H. Kim, Prof. Dr. E. Kim
Department of Chemical and Biomolecular Engineering
Yonsei University
50 Yonsei-ro, Seodaemun-gu, Seoul 120-749 (Korea)
E-mail: jonghak@yonsei.ac.kr
eunkim@yonsei.ac.kr
Homepage: http://web.yonsei.ac.kr/eunkim
Dr. J. Kim,[+] J. K. Koh,[+] B. Kim, Prof. Dr. J. H. Kim, Prof. Dr. E. Kim
Active Polymer Center for Pattern Integration (APCPI)
Yonsei University
50 Yonsei-ro, Seodaemun-gu, Seoul 120-749, (Korea)
[+] These authors contributed equally to this work.

[**] We acknowledge financial support from a National Research Foundation (NRF) grant funded by the Korean government (MEST) through the Active Polymer Center for Pattern Integration (R11-2007-050-00000-0).
Supporting information for this article is available on the WWW under http://dx.doi.org/10.1002/anie.201202428.

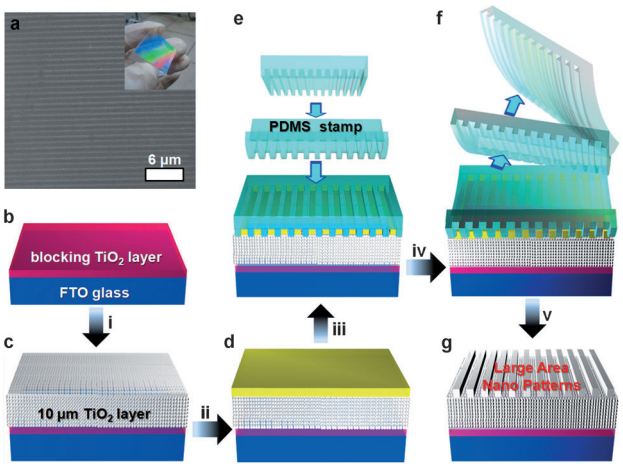

Figure 1. The nanopatterning process for the TiO_2 photoelectrode. a) SEM image of the PDMS stamp (inset: photograph of the PDMS stamp, 2.4 cm × 2.4 cm). b,c) The general process for the preparation of a thick photoelectrode from acidic paste; d) coating the neutral paste on a thick TiO_2 layer; e)–g) the soft nanopatterning process using the PDMS stamp. i) doctor-blade coating of acidic paste and calcination at 450 °C; ii) doctor-blade coating of neutral paste; iii),iv) nanopatterning using the PDMS stamp, drying, and detachment; v) annealing after detachment and calcination at 450 °C. See the text for details.

ing Information, Figure S2a). Poor dye adsorption resulted because of the mismatch between the hydrophobic TiO_2 surface and hydrophilic N719 dye solution (Figure 2d,e). Alternatively, the patterned photoelectrode prepared with a neutral TiO_2 paste had a hydrophilic nature, which is more appropriate for successful dye adsorption. Similar phenomena were also observed in the mesoporous TiO_2 films with 20 μm line micropatterning (Supporting Information, Figure S1c,d). These observations were confirmed by a surface characterization, SEM, and FTIR spectroscopic analysis (see Figure 2b–e; Supporting Information, Figures S1, S2 and detailed discussions). We prepared an 11 μm-thick, double-layered photoelectrode using acidic (first thick layer = 10 μm) and neutral pastes (second thin nanopatterned layer < 1 μm) through a two-step casting method (Figure 1; Supporting Information, Videos S1, S2).

The single-layered photoelectrode prepared with the neutral paste resulted in lower efficiency owing to the reduced thickness. The increase in the thickness of the TiO_2 film prepared from a neutral paste led to crack formation. The first thick TiO_2 layer prepared with an acidic paste was about 400 nm, whereas the second thin layer from the neutral paste contained 20 nm NPs (Figure 3a,b).

After patterning and then calcination at 450 °C, the surface was homogeneous without crack formation or physical delamination, as shown in the SEM images (Figure 3b–f). Although there were no defects over a large area (Figure 3c), the projected pattern size was reduced in all directions, that is, width (from ca. 300 to ca. 250 nm) and height (from ca. 190 to ca. 50 nm), as a result of the burn-out of the organic binder (Figure 3c inset and 3d). The changes in pattern size were confirmed using atomic force microscopy (AFM) analysis (Figure 3g–j), and the results were consistent with the SEM results. Paste residue was not observed on the PDMS stamp when the stamp was removed (Supporting Information, Video S2). Thus, the stamp could be successfully reused several times for subsequent patterning processes (Figure 3f and inset), demonstrating that this is a reproducible, inexpensive, and effective method. Moreover, this patterning method using a PDMS stamp could be applied to micropatterning processes with various pattern shapes and sizes (Supporting Information, Figure S3), indicating its universality.

Iodine-free ssDSSCs were constructed with SnO_2/F-layered (FTO) glass, a dense TiO_2 blocking layer, an N719-dye-adsorbed nanocrystalline 10 μm-thick TiO_2 layer, a < 1 μm-thick nanopatterned layer, a conductive PEDOT, and a Pt-coated counterelectrode (Figure 2a).[27] A solution containing a solid-state polymerizable monomer, 2,5-dibromo-3,4-ethylenedioxythiophene (DBEDOT), was directly cast on the dye-adsorbed TiO_2 photoelectrode, followed by thermal polymer-

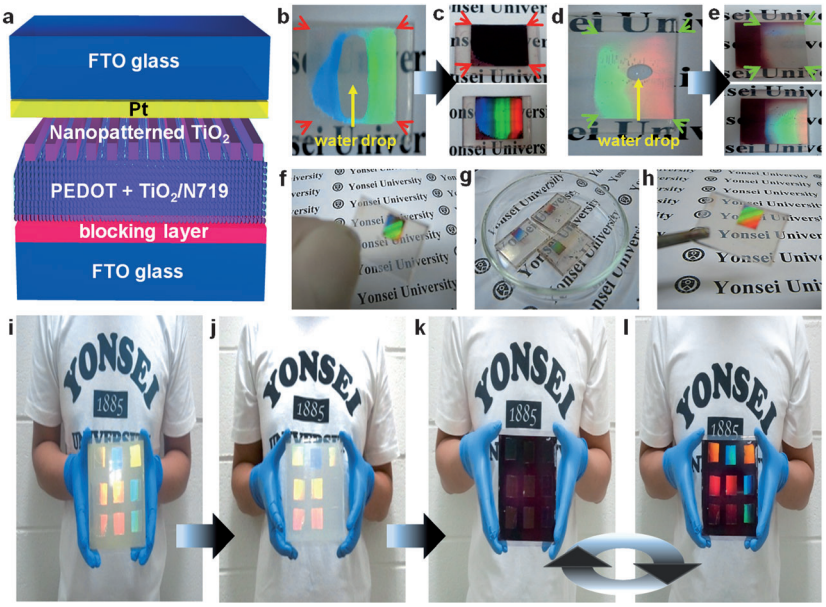

Figure 2. The structure of I_2-free ssDSSCs, with nanopatterns and photographs of the fabrication process and large-area-patterned photoelectrodes. a) The fabricated cell structure with nanopatterns and conductive polymer. b), d) Hydrophilicity analyzed by a water drop test on the nanopatterned photoelectrode prepared from b) neutral and d) acidic pastes. c), e) Photographs of dye-adsorbed photoelectrodes prepared from c) neutral and e) acidic pastes. f)–h) Photographs of the f) dye adsorption and g), h) solid-state polymerization of PEDOT. i) Large-area patterning and drying of neutral paste on the first layer, j) after calcination, k) after N719 dye adsorption, l) Photograph of the fabricated large area photoelectrode at a different viewing angle to (k); see the Supporting Information, Video S3.

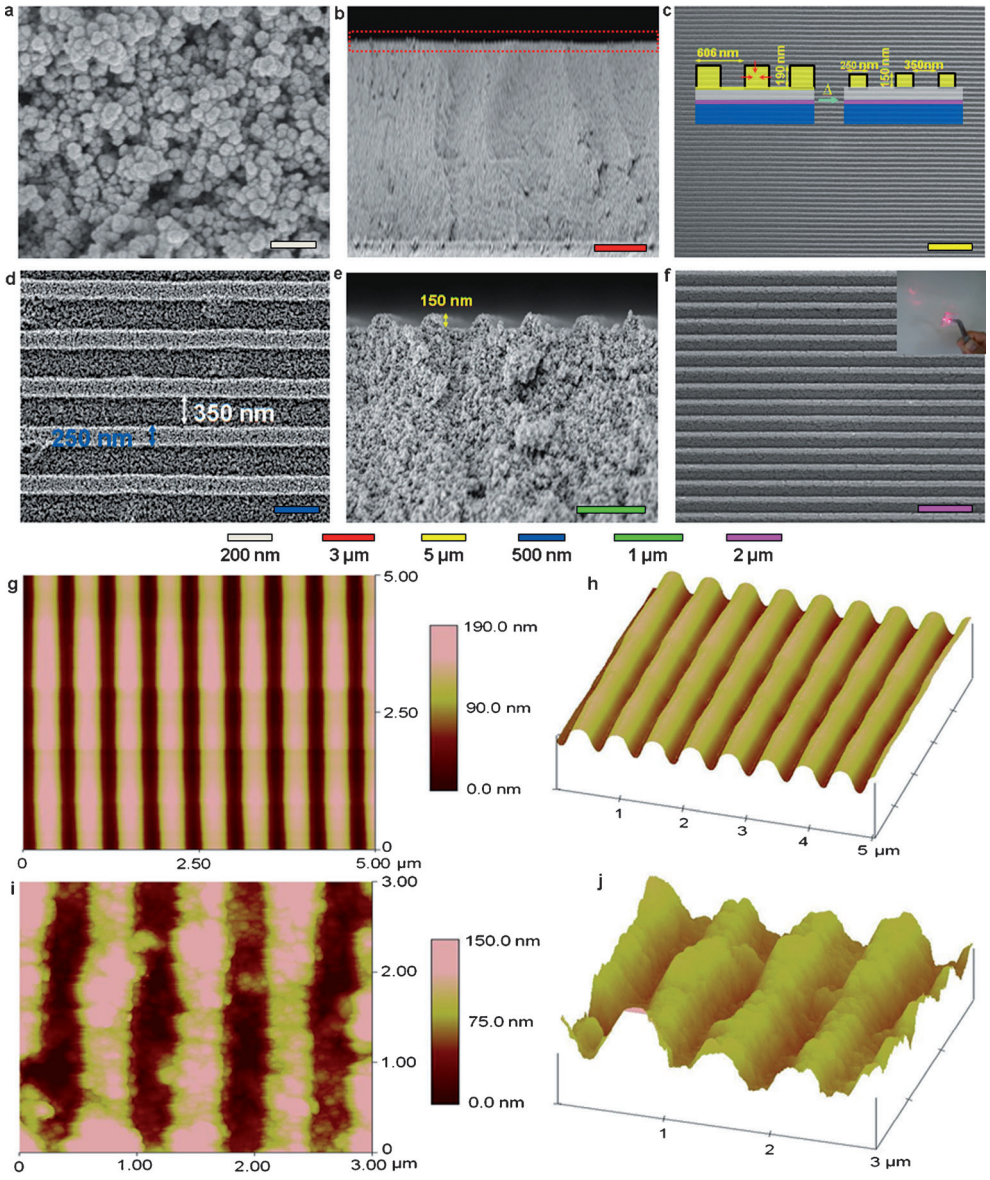

Figure 3. SEM and AFM images of the TiO_2 layer and nanopatterned photoelectrodes. a) The top surface of the 10 μm TiO_2 layer prepared from acidic paste. b) Cross-section of the nanopatterned TiO_2 layer after nanopatterning of the neutral paste on (a). c)–e) One-dimensional periodic line nanopatterns on c), d) the top and e) the cross-section. f) The periodic line TiO_2 nanopatterns formed using the PDMS stamp (reusability). g), h) AFM images of the fabricated master PDMS. i), j) AFM images of the nanopatterned photoelectrode. Insets: c) shrinkage of the pattern by calcination after patterning and drying; f) photograph of the diffraction test of the nanopatterned photoelectrode using a 632 nm laser.

ization at 50–60 °C to produce a conducting PEDOT (Figure 2 f–h). Even after dye adsorption and polymerization, the photoelectrode stayed intact so that the reflected and diffracted light can induce effective light harvesting in solar cells.

Multipatterned photoelectrodes with good reflective properties were prepared over a large area (400 cm^2) of FTO glass using nine stamps in a single step, indicating its scalable processability (Figure 2 i–l; Supporting Information, Video S3). Figure 4 a depicted light reflection from the nanopatterned TiO_2 photoelectrode.

When periodic line patterns are deposited on the photoelectrode layer, the incident light reaching the grating can be diffracted in a backward direction. The angle of the diffracted light can be determined from the following equation [Eq (1)]:[1]

$$m\lambda = n_{active}\, p\, (\sin\theta_i + \sin\theta_d) \quad (1)$$

where n_{active} is the refractive index of the nanocrystalline TiO_2 layer, p is the period of the grating, m is the order of the diffracted light, λ is the wavelength of the incident light, and θ_i and θ_d are the incidence and diffraction angles, respectively. The n_{active} of the mesoporous TiO_2 film was determined to be about 2.256 (21 % porosity)[31] and p is 600 nm in our nanopattern. For $250\ nm \le \lambda \le 600\ nm$ and $600\ nm \le \lambda \le 760\ nm$, a diffracted light can have m values of 0, ± 1, and ± 2 and m values of 0 and ± 1, respectively. At higher m values, the θ_d of the diffracted light can be bent by 90°, which cannot be absorbed through the dye-adsorbed TiO_2 layer. The incident light of $\lambda = 250$ and 760 nm has a θ_d of 10.6 and 34.2° for the first-order reflection, respectively, and incident light of $\lambda = 250$ and 676 nm has a θ_d of 21.7 and 87.2° for the second-order reflection, respectively. In contrast to smaller period nanopatterns, the nanopatterned TiO_2 film with $p = 600$ nm can effectively absorb nearly all of the light diffracted backwards in the absorbance range of N719 dye. It is important that the diffracted backwards light of $m = 1$ can have a θ_d of 90° under $p = 300$ nm at $\lambda = 676$ nm that cannot be absorbed by N719 dye. Therefore, the periodic nanopatterns on the top of the photoelectrode can reflect the light back to the photoelectrode again, and thus enhance the optical path length across a broad wavelength range of incident light, leading to further light absorption. The optical properties of the fabricated photoelectrodes were characterized to investigate the light harvesting ability. The reflection

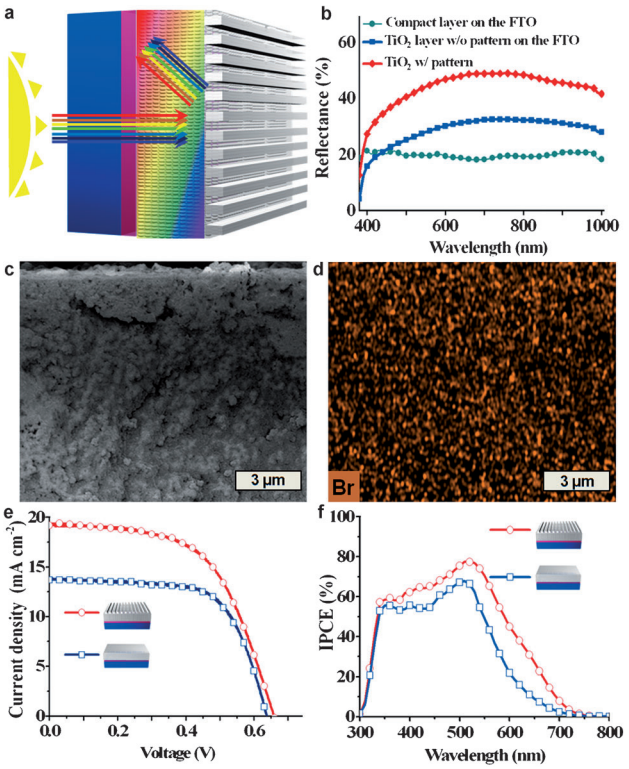

Figure 4. Comparison of the reflection for light trapping and the cell performance, and evidence of effective penetration of the conductive polymer HTM. a) Light trapping on the nanopatterned TiO_2 layer. b) The reflection behaviors of the compact (blocking layer), flat, and nanopatterned TiO_2 layers on the FTO substrate. c) Cross-sectional SEM image of the N719 dye adsorbed to the TiO_2 photoelectrode after DBEDOT penetration and polymerization. d) EDS mapping of the Br element of (c) from Br_3^--doped PEDOT. e) Photocurrent density–voltage curves of each cell at AM 1.5 G, one sun illumination. f) IPCE spectra of each cell.

spectra of each sample are shown from the 400 to 1000 nm wavelengths in Figure 4b. The dense, compact TiO_2 layer on the FTO showed circa 20% reflectance over the whole range, whereas the flat TiO_2 layer without a pattern exhibited 20–30% reflectance in the visible range, indicating less-effective light trapping. In contrast, the TiO_2 film with the nanopattern exhibited high reflection of light with 30–50% over the whole range, which is approximately 20% greater than the flat TiO_2 layer and provides strong evidence of the light harvesting effect of nanopatterning. The DSSC fabricated with nanopatterning showed a high level reflection of the 635 nm light, whereas DSSCs without nanopatterning or with micropatterning were not effective in capturing the light owing to poorer reflection properties (Supporting Information, Figure S4).

Good interfacial contact between the electrode and electrolyte is pivotal for enhancing the efficiency of I_2-free ssDSSCs.[27,28] Deep penetration of a solid conducting polymer into the TiO_2 nanopores was directly observed using energy-dispersive X-ray spectrometry (EDS) mapping (Figure 4d; Supporting Information, Figure S5). Bromine from the dopant (Br_3^-) of PEDOT was uniformly dispersed throughout the 11 μm-thick mesoporous TiO_2 films, indicating good pore filling by PEDOT.

Cell parameters determined from the current density versus voltage (J–V) curves and electrical impedance spectroscopy (EIS; Figure 4e; Supporting Information, Figure S6) are summarized in Table 1 and the Supporting Information, Table S1, respectively. The photoconversion efficiency of the DSSC with nanopatterns reached 7.03% at 100 mW cm^{-2}, which is approximately 33% greater than that that without nanopatterns. The improvement in efficiency is mostly due to the approximate 40% increase in the J_{sc} value. A slightly lower FF of the DSSC with nanopatterns might be due to a slightly increased film thickness and PDMS stamping-induced densified structure, leading to the increased difficulty of solid-state electrolyte infiltration into the pores. Incident photon-to-current efficiency (IPCE) curves of the DSSCs were measured at a chopper frequency of 5 Hz in alternating-current mode (Figure 4f). The J_{sc} values determined from the IPCE curves were consistent with those from the J–V curves within 5% error. In the wavelength region of 350–800 nm, the DSSC with nanopatterns produced greater IPCE values than that without nanopatterns, indicating that the nanopatterned layer conferred improved light-utilization efficiency.

In conclusion, we have developed a simple, fast, and universal nanopatterning methodology for boosting the light harvesting efficiency of DSSCs based on a light-trapping technique. We achieved performance enhancements of 40% J_{sc} and 33% η in I_2-free ssDSSCs, reaching 7.03% at 100 mW cm^{-2}, which is one of the highest values reported for I_2-free ssDSSCs to date. Our approach with direct nanopatterning of TiO_2 films is scalable to large areas and compatible with mass production as it is easy and inexpensive, reusable, and most importantly, universally applicable to a variety of solar cells utilizing inorganic oxides, quantum dots, or organic materials. This method shows promise for facilitating the manufacture of solar cells with remarkable light harvesting ability. Furthermore, this patterning process including nanometer- and micrometer-sized patterns and various shapes of nanoparticles can be used for desired applications.

Experimental Section

Nanopatterning of TiO_2 films: The dense, compact TiO_2 blocking layer (Figure 1b) with a 200 nm thickness was prepared by spin-coating a titanium bis(ethyl acetoacetate) solution (2 wt% in butanol) onto FTO glass (Pilkington. Co. Ltd., 8 Ω/□) at 2000 rpm for 30 s, followed by calcination at 450°C for 30 min. Commercially available acidic TiO_2 paste (Ti-Nanoxide D20, Solaronix S.A., Switzerland) was cast onto the compact TiO_2 layer using a doctor-blade technique and dried at 50°C for 30 min. After successive sintering at 450°C for 30 min and cooling to 30°C for 8 h, nanocrystalline TiO_2 films with a thickness of 10 μm were obtained (Figure 1c). The commercially available neutral paste (TiO_2 Paste DSL 18NR-T, Dyesol, Australia) was doctor-bladed to form a thin layer directly on top of the 10 μm-thick nanocrystalline TiO_2 layer (Figure 1d) and then the PDMS stamp was manually placed on a neutral paste-coated photoelectrode with proper pressure (Figure 1e; Supporting Information, Video S1). The photoelectrode was maintained at 25°C for 16 h and the stamp was peeled off (Figure 1e,f; Supporting Information, Video S2). The nanopatterned

photoelectrode was annealed at 60–70 °C for 3 h and sintered under the same conditions. Large photoelectrodes with nanopatterns were prepared by the same conditions using FTO glass (20 cm × 20 cm) and replica stamps (Figure 3i–l). The used PDMS was washed with ethanol and could be reused.

DSSC fabrication: The nanopatterned photoelectrode was immersed in the N719 dye (Solaronix SA, Switzerland) solution (0.5 mM in ethanol) for 24 h at room temperature, washed with ethanol, and dried. For the pore-filling of HTM, the synthesized monomer (DBEDOT) was dissolved in anhydrous ethanol. One drop of dilute solution (1 wt%) was cast and dried under ambient conditions. One drop of a more concentrated solution (3 wt%) in ethanol was directly cast onto the photoelectrode, and then dried under the same conditions. This process was also repeated three times. After complete drying of the solvent, the DBEDOT-incorporated photoelectrode was put into a vial and capped, then thermally polymerized at 55 °C for 24 h in an oven to produce a highly conductive polymer (PEDOT). One drop of the ethanol solution consisting of 1-methyl-3-propylimidazolium iodide (1.0 M, MPII, Aldrich Chemicals), 4-*tert*-butylpyridine (0.2 M, TBP, Aldrich Chemicals), and lithium bis(trifluoromethane)sulfonimide (0.2 M, LiTFSI, Aldrich Chemicals) was cast onto the dye-sensitized TiO_2 photoelectrode with conductive polymers. After complete evaporation of the solvent in a vacuum oven, sandwich-type ssDSSCs were fabricated through the attachment of the Pt-coated counterelectrode and sealing. The active area was 0.16 cm^2.

Received: March 28, 2012
Published online: June 8, 2012

Keywords: dye-sensitized solar cells · light harvesting · nanopatterning · photoanodes · TiO_2 nanoparticles

[1] S.-I. Na, S.-S. Kim, J. Jo, S.-H. Oh, J. Kim, D.-Y. Kim, *Adv. Funct. Mater.* **2008**, *18*, 3956 – 3963.
[2] C. Battaglia, J. Escarré, K. Söderström, M. Charrière, M. Despeisse, F.-J. Haug, C. Ballif, *Nat. Photonics* **2011**, *5*, 535 – 538.
[3] N. Ozawa, H. Yabe, T. Yao, *J. Am. Ceram. Soc.* **2003**, *86*, 1976 – 1978.
[4] J. S. Kim, Y. Park, D. Y. Lee, J. H. Lee, J. H. Park, J. K. Kim, K. Cho, *Adv. Funct. Mater.* **2010**, *20*, 540 – 545.
[5] S. Guldin, S. Hüttner, M. Kolle, M. E. Welland, P. Müller-Buschbaum, R. H. Friend, U. Steiner, N. Tétreault, *Nano Lett.* **2010**, *10*, 2303 – 2309.
[6] D.-H. Ko, J. R. Tumbleston, W. Schenck, R. Lopez, E. T. Samulski, *J. Phys. Chem. C* **2011**, *115*, 4247 – 4254.
[7] I.-K. Ding, J. Zhu, W. Cai, S.-J. Moon, N. Cai, P. Wang, S. M. Zakeeruddin, M. Grätzel, M. L. Brongersma, Y. Cui, M. D. McGehee, *Adv. Eng. Mater.* **2011**, *1*, 52 – 57.
[8] J. N. Munday, H. A. Atwater, *Nano Lett.* **2011**, *11*, 2195 – 2201.
[9] B. O'Regan, M. A. Grätzel, *Nature* **1991**, *353*, 737 – 740.
[10] K. Zhu, T. B. Vinzant, N. R. Neale, A. J. Frank, *Nano Lett.* **2007**, *7*, 3739 – 3746.
[11] T. Krishnamoorthy, V. Thavasi, M. Subodh, G. S. Ramakrishna, *Energy Environ. Sci.* **2011**, *4*, 2807 – 2812.
[12] a) Z. Sun, J. H. Kim, Y. Zhao, F. Bijarbooneh, V. Malgras, Y. Lee, Y.-M. Kang, S. X. Dou, *J. Am. Chem. Soc.* **2011**, *133*, 19314 – 19317; b) S. H. Kim, Y. N. Kim, J. M. You, J. Y. Lee, E. Kim, *Korean J. Imag. Sci. Tech.* **2010**, *16*, 11 – 16.
[13] B. E. Hardin, E. T. Hoke, P. B. Armstrong, J.-H. Yum, P. Comte, T. Torres, J. M. J. Fréchet, M. K. Nazeeruddin, M. Grätzel, M. D. McGehee, *Nat. Photonics* **2009**, *3*, 406 – 411.
[14] T. Bessho, S. M. Zakeeruddin, C.-Y. Yeh, E. W.-G. Diau, M. Grätzel, *Angew. Chem.* **2010**, *122*, 6796 – 6799; *Angew. Chem. Int. Ed.* **2010**, *49*, 6646 – 6649.
[15] A. Hagfeldt, G. Boschloo, L. Sun, L. Kloo, H. Pettersson, *Chem. Rev.* **2010**, *110*, 6595 – 6663.
[16] A. Yella, H.-W. Lee, H. N. Tsao, C. Yi, A. K. Chandiran, Md. K. Nazeeruddin, E. W.-G. Diau, C.-Y. Yeh, S. M. Zakeeruddin, M. Grätzel, *Science* **2011**, *334*, 629 – 634.
[17] T. Daeneke, T.-H. Kwon, A. B. Holmes, N. W. Duffy, U. Bach, L. Spiccia, *Nat. Chem.* **2011**, *3*, 211 – 215.
[18] For selective positioning of organic dyes in a mesoporous inorganic oxide film, see: K. Lee, S. W. Park, M. J. Ko, K. Kim, N.-G. Park, *Nat. Mater.* **2009**, *8*, 665 – 671.
[19] A. Nattestad, A. J. Mozer, M. K. R. Fischer, Y.-B. Cheng, A. Mishra, P. Bäuerle, U. Bach, *Nat. Mater.* **2010**, *9*, 31 – 35.
[20] Q. Miao, L. Wu, J. Cui, M. Huang, T. Ma, *Adv. Mater.* **2011**, *23*, 2764 – 2768.
[21] A. Mihi, C. Zhang, P. V. Braun, *Angew. Chem.* **2011**, *123*, 5830 – 5833; *Angew. Chem. Int. Ed.* **2011**, *50*, 5712 – 5715.
[22] C. T. Yip, H. Huang, L. Zhou, K. Xie, Y. Wang, T. Feng, J. Li, W. Y. Tam, *Adv. Mater.* **2011**, *23*, 5624 – 5628.
[23] L. Yang, W. W.-F. Leung, *Adv. Mater.* **2011**, *23*, 4559 – 4562.
[24] S.-H. Han, S. Lee, H. Shin, H. S. Jung, *Adv. Energy Mater.* **2011**, *1*, 546 – 550.
[25] M. Wang, X. Pan, X. Fang, L. Guo, W. Liu, C. Zhang, Y. Huang, L. Hu, S. Dai, *Adv. Mater.* **2010**, *22*, 5526 – 5530.
[26] H. Tokuhisa, P. T. Hammond, *Adv. Funct. Mater.* **2003**, *13*, 831 – 839.
[27] J. K. Koh, J. Kim, B. Kim, J. H. Kim, E. Kim, *Adv. Mater.* **2011**, *23*, 1641 – 1646.
[28] J. Kim, J. K. Koh, B. Kim, S. H. Ahn, H. Ahn, D. Y. Ryu, J. H. Kim, E. Kim, *Adv. Funct. Mater.* **2011**, *23*, 4168 – 4173.
[29] M. J. Allen, V. C. Tung, L. Gomez, Z. Xu, L.-M. Chen, K. S. Nelson, C. Zhou, R. B. Kaner, Y. Yang, *Adv. Mater.* **2009**, *21*, 2098 – 2102.
[30] S. M. Kim, S. J. Ku, J. B. Kim, *Macromol. Res.* **2011**, *19*, 891 – 896.
[31] D. Parralejoa, R. Carusob, A. L. Ortiza, F. Guiberteau, *Thin Solid Films* **2004**, *458*, 92 – 97.

